Sensitivity Enhancement for Fiber Bragg Grating Strain Sensing Based on Optoelectronic Oscillator with Vernier Effect

Xiaozhong Tian, Jingzhan Shi, Yiping Wang, Le Li and Yun She

***Abstract*—Based on a dual-loop optoelectronic oscillator (OEO) with Vernier effect, a scheme of fiber Bragg grating (FBG) interrogation system with an improved scale factor has been proposed and experimentally demonstrated. Functioning as the optical carrier of the OEO, the reflection signal of two cascaded FBGs is divided into two optical beams by using a wavelength division multiplexer (WDM). The two optical beams at different wavelengths travel along single mode fibers with different lengths. After combined together by another WDM, the two optical beams go through a section of dispersion compensation fiber (DCF). The oscillating frequency shift of the OEO is determined by the overall time delay, which is affected by the wavelength change of the sensing FBG. Thus, the wavelength change of the sensing FBG can be converted into the oscillating frequency shift of the OEO. Furthermore, due to the length difference between the two optical beams, an obvious Vernier effect has been generated in the frequency response of the OEO. By detecting the frequency shift of the envelope peak of the frequency response curve, the sensitivity of the sensing interrogation can be enhanced greatly. A proof-of-concept OEO-based FBG sensor for axial strain sensing experiment is performed. The experimental results show that the sensitivity is about 0.31 KHz/με for a single-loop OEO. By employing Vernier effect, the sensitivity can be improved to -11 KHz/με, which is 35 times higher than that of the single-loop OEO.**

***Index Terms*—Bragg gratings, microwave oscillators, optoelectronic and photonics sensors, optical sensors.**

I. Introduction

During the last few decades, fiber Bragg grating (FBG) sensors have been considered a promising sensing technology and have been investigated extensively due to their intrinsic advantages, including immunity to electromagnetic interference, compact size, low weight and unique wavelength multiplexing capability [1]. The operation of FBG sensors is that their reflection or transmission spectrum is affected by physical parameter to be measured. Their inherent wavelength-encode strain/temperature response makes them easy to interrogate and multiplex. However, the most common approaches to interrogate the FBG sensor tend to rely on the use of optical spectrum analyzer (OSA), optical filter, a tunable laser or an optical interferometer, which is implemented in the optical domain. However, it usually suffers from poor resolution and low speed [2]. Therefore, it is desirable to develop FBG sensors with high resolution and fast speed for high-performance sensing applications.

As a typical optoelectronic hybrid oscillator, optoelectronic oscillator (OEO) was proposed originally for the purpose of generating high frequency microwave signal with high spectrum purity and low phase noise [3]. By applying OEO to optical fiber sensing, the resolution and interrogating speed can be improved effectively [4, 5]. The fundamental concept of using an OEO for optical fiber sensing is to convert the sensing parameters into the frequency change of the OEO generated microwave signal. Benefiting from the features, numerous OEO-based optical fiber sensors have been proposed for optical fiber length [6], temperature [7, 8] refractive index [9] sensing and so on. Among the various structures, OEO-based FBG sensors, with advantages of simplest structure and interrogation scheme, have attracted significant attention. OEO-based FBG sensors can be divided into two categories. The fundamental principle behind the first category is inspired from the operating principle of a microwave photonics bandpass filter (MPF). The frequency shift on MPF inserted in OEO can be affected by FBG sensors, which is sensitive to detecting physical parameters. Based on this principle, several interrogation systems have been proposed to detect refractive index [10, 11], pressure [12], axial strain and temperature [13, 14]. The oscillating frequency of the OEO is determined by the overall time delay of the loop, which will be affected by the wavelength change of the sensing FBG. According to this concept, another approach to implement an OEO-based FBG sensor has been proposed for position location [15], axial strain detection [16] and magnetic field measure [17]. In [16], an interrogation scheme for normal FBG sensors employing an OEO loop containing a dispersive medium have been proposed. The sensitivity is about 58 Hz/με, which will not satisfy some requirements of extremely small axial strain measurements. In [17], a magnetic field sensor based on two OEOs incorporating cascaded magnetostrictive alloy-fiber Bragg grating (MA-FBG) and FBG filters have been demonstrated. The second FBG is

This work was supported by the National Natural Science Foundation of China under Grant 61975082 and 62101269; (Corresponding author: Yiping Wang)

Xiaozhong Tian, Jingzhan Shi, Yiping Wang, Le Li and Yun She are with Jiangsu Key Lab on Opto-Electonic Tecnology, School of Computer and Electronic Information, Nanjing Normal University, Nanjing 210023, China. (Email: tianxiaozhong19@126.com, shijz@nnu.edu.cn, jeremy_ff@sina.com, 1532910624@qq.com, 997037657@qq.com)

used to separate two measurands and the sensitivity for magnetic field and temperature are about 250 Hz/Oe and 1.97 or 1.42 Hz/℃. Even though the cross-sensitivity is solved, the sensitivity is not improved significantly and two OEOs in the system increase the cost and complexity. Recently, to further improve OEO-based optical fiber sensors' sensitivity, the Vernier effect is introduced [18]. However, to the best of our knowledge, an OEO-based FBG sensor with Vernier effect has never been reported.

In this paper, a scheme of OEO-based FBG sensor with an improved scale factor by employing Vernier effect is proposed and experimental demonstrated. In the proposed system, the optical carrier is provided by the reflection signal of two cascaded FBGs with different resonance wavelengths. The optical carrier is divided into two optical beams via a wavelength division multiplexer (WDM) and then send to single mode fibers (SMF) with slightly different lengths. After combined together by another WDM, the two optical beams travel along a roll of dispersion compensation fiber (DCF) together, which is working as the dispersion element in the OEO loop. The oscillating frequency of the OEO is determined by the overall time delay, which is a related to the wavelength of the optical carrier. Hence, the resonance wavelength change of the sensing FBG can be converted into the oscillating frequency shift of the OEO. Because of the length difference in two optical beams, an obvious Vernier effect has been generated in the frequency response of the OEO. With the advantages of Vernier effect, the shift of envelope is more distinct, making the sensor's sensitivity enhance greatly and measurement error reduce enormously.

II. Analytical Analysis

The proposed OEO-based FBG sensor interrogation system is schematically shown in Fig. 1. The light emits from an amplifier spontaneous emission source (ASE) is sent to the two cascaded FBGs through port 1 of an optical circulator (OC). The resonance wavelengths of two cascaded FBGs are λ_{FBG1} and λ_{FBG1} respectively. Working as the optical carrier, the reflection signal of two cascaded FBGs is injected into a Mach-Zehnder (MZM) via a polarization controller (PC). The modulated light wave out of the MZM is amplified by the Erbium-doped fiber amplifier (EDFA) and then sent to a wavelength division multiplexer (WDM). The light is divided into two paths by WDM 1 according to the wavelengths. Two optical paths go through two sections of signal mode fibers (SMF) with different lengths. The two optical paths are combined together by WDM 2 and are then injected into a roll of dispersion compensation fiber (DCF), which working as the dispersion element in the OEO loop. The total optical signal is converted to the electrical signal by a PD. The corresponding electrical signal is amplified by an electrical amplifier (EA). After selected by a microwave bandpass filter (BPF), the electrical signal is fed back to the MZM via one outlet of the electrical coupler (EC) to make the OEO loop closed. The other outlet of the EC is analyzed with an electrical spectrum analyzer (ESA).

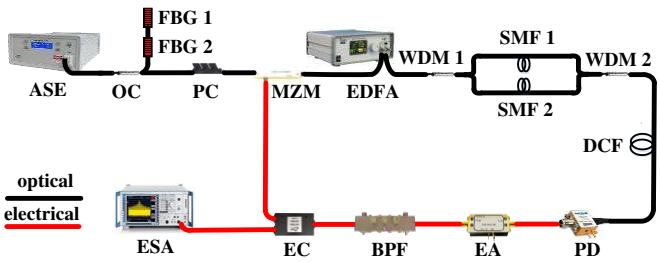

Fig. 1. Schematic of the proposed OEO based FBG sensor (ASE: amplified spontaneous emission; OC: optical circulator; FBG: fiber Bragg grating; PC: polarization controller; MZM: Mach-Zehnder modulator; WDM: wavelength division multiplexer; SMF: single mode fiber; DCF: dispersion compensation fiber; PD: photodetector; EA: electrical amplifier; BPF: bandpass filter; EC: electrical coupler; ESA: electrical spectrum analyzer)

It is known that the resonance wavelength of FBG shift linearly with the axial strain applied to it. Since two FBGs are grouped into a room temperature environment, the influence of temperature can be ignored. Thus, the wavelength response of the axial strain can be written as:

$$\Delta\lambda_{\mathrm{FBG}} = K_{\varepsilon} \cdot \varepsilon \cdot \lambda_{\mathrm{FBG}} \tag{1}$$

Where K_{ε} and ε represent the axial strain coefficient and the applied axial strain, respectively.

According to the working principle of the OEO, the microwave frequency generated by OEO is determined by the overall time delay of the loop. As presented in Fig. 1, the overall time delay (t) in the OEO loop consists of optical link and electrical link, which can be expressed as:

$$t_{1,2} = t_{\mathrm{o}_{1,2}} + t_{\mathrm{e}} = t_{\mathrm{e}} + \frac{n_{\mathrm{SMF}} L_{\mathrm{SMF}_{1,2}} + n_{\mathrm{DCF}} L_{\mathrm{DCF}}}{c} \tag{2}$$

Where t_{e} and t_{o} stand for the time delay induced by the electrical link and the optical link respectively. L_{SMF} and L_{DCF} represent the length of the SMF and DCF, respectively. n_{SMF} and n_{DCF} are the effective refractive indexes of the SMF and DCF, respectively. c is the velocity of light. The subscript indicates loop 1 and loop 2.

The free spectrum range (FSR) and the frequency of the N^{th} harmonic are:

$$FSR_{1,2} = \frac{1}{t_{1,2}} \tag{3}$$

$$f_{N_{1,2}} = N_{1,2} \cdot FSR_{1,2} = \frac{N_{1,2}}{t_{1,2}} \tag{4}$$

Obviously, t will change with the wavelength shift of FBG. Since the dispersion of SMF is much smaller than that of DCF, and the length of SMF is relatively short comparing with that of DCF, the time delay variation caused by SMF can be ignored. The time delay Δt can be given:

$$\Delta t = D \cdot L_{\mathrm{DCF}} \cdot \Delta\lambda_{\mathrm{FBG}} \tag{5}$$

Where D is the dispersion of DCF. Therefore, the oscillating frequency shift Δf of f_N can be expressed as:

This article has been accepted for publication in a future issue of this journal, but has not been fully edited. Content may change prior to final publication. Citation information: DOI 10.1109/JPHOT.2021.3119960, IEEE Photonics Journal

$$\Delta f_{1,2} = N_{1,2} \cdot \Delta FSR_{1,2} = \frac{N_{1,2}}{t_{1,2} + \Delta t} - \frac{N_{1,2}}{t_{1,2}} \approx -\frac{N_{1,2}\Delta t}{t_{1,2}^{\,2}}, \quad (\Delta t \ll t_{1,2}) \tag{6}$$

Applying Eqs. (1)-(5) to Eq. (6), the relationship between Δf and ε can be reduced as:

$$\Delta f_{1,2} = -\frac{N_{1,2} D L_{\mathrm{DCF}} K_{\varepsilon} \varepsilon \lambda_{\mathrm{FBG}}}{\left[t_{\mathrm{e}} + \frac{n_{\mathrm{SMF}} L_{\mathrm{SMF}_{1,2}} + n_{\mathrm{DCF}} L_{\mathrm{DCF}}}{c} \right]^2} \tag{7}$$

Seen from Eq. (7), the oscillating frequency shift is proportional to the axial strain applied to the FBG. Meanwhile, the measurement accuracy can be enhanced greatly by adopting high-order oscillating frequency modes.

To improve the sensor's sensitivity, Vernier effect is achieved by adjusting suitable lengths of SMF 1 and SMF 2 in the OEO loop. Based on the principle of Vernier effect [19, 20], the FSR of the dual loop OEO (FSR_d) and the frequency of the envelop peak at $N_d^{\,th}$ harmonic (f_{N_d}) can be described as follows:

$$FSR_d = \frac{FSR_1 \times FSR_2}{\left| FSR_1 - FSR_2 \right|} \tag{8}$$

$$f_{N_d} = N_d \cdot FSR_d \tag{9}$$

Where $N_d = N_{1,2} \times \left| FSR_2 - FSR_1 \right| / FSR_{2,1}$ .Therefore, the oscillating frequency shift Δf_d of f_{N_d} can be expressed as:

$$\Delta f_d = N_d \cdot \Delta FSR_d \tag{10}$$

In comparison, the oscillating frequency shift between single-loop OEO and dual-loop OEO with Vernier effect can be reduced as:

$$\frac{\Delta f_{\mathrm{d}}}{\Delta f_{1,2}} \approx -\frac{FSR_{2,1}}{\left| FSR_2 - FSR_1 \right|}, \quad (\Delta FSR_{1,2} \ll FSR_{1,2}) \tag{11}$$

As can be seen from Eq. (11), the dual-loop OEO have a significantly enhanced frequency shift as compared with that of a single-loop OEO when there is a slightly difference between FSR_1 and FSR_2 . Meanwhile, the frequency response of dual-loop OEO shifts to the opposite direction compared with that of single-loop OEO.

III. Experimental Setup and Result

To verify the proposed OEO-based FBG sensor interrogation system, an experiment is carried out based on the setup shown in Fig. 1. The resonance wavelengths of two FBGs are 1535.036 nm with a bandwidth of 0.25 nm and 1555.268 nm with a bandwidth of 0.25 nm, respectively. The MZM (Photline, MX-LN-20) has a 20 GHz bandwidth and half-wave voltage of 5.5 V. The maximum output power of the EDFA (Amonics, AEDFA-IL-18-B-FA) is 18 dBm. A single mode fiber patch cord with a length of 20 m is inserted in SMF 1. Thus, the length difference between L_{SMF1} and L_{SMF2} is 20 m. The length of DCF is 600 m and the dispersion is about -188 ps/nm·Km. Hence, the total dispersion of the DCF is -112.8 ps/nm. The bandwidth of PD (FINISAR, XPDV2120RA) is 50 GHz. The center frequency and bandwidth of the BPF are 9 GHz and 60 MHz. The ESA (R&S, FSV-30) has a measurement range of 0-30 GHz.

For the axial strain measurement, the FBG with a resonance wavelength of 1535.036 nm is used as an axial strain sensor. The sensing FBG is fixed by two fiber clamps fixed to the slide platform. The axial strain is applied to the FBG by moving the stage at room temperature.

Firstly, we measure the wavelength response of the sensing FBG to axial strain in optical domain by OSA (YOKOGAWA, AQ6370D) with a resolution of 0.02 nm, showing in Fig. 2. During this test, the axial strain is applied to the sensing FBG from 0-956 με with a step of 27 με. Both the axial strain increase and decrease experiment are performed. As can be seen from Fig. 2, the resonance wavelength of the sensing FBG increases with the axial strain increases, while the resonance wavelength of the sensing FBG decreases with the axial strain decreases. According to the linear fitted line, the sensitivity of the sensing FBG is 1.1 pm/με.

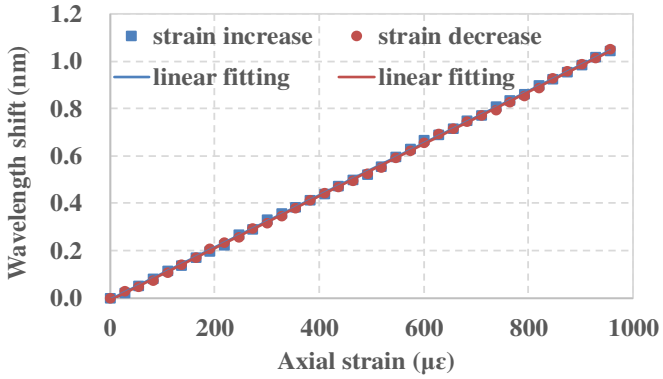

Fig. 2. The relationship between the resonance wavelength of the sensing FBG and the applied axial strain.

Secondly, the characteristic of Vernier effect generated in dual-loop OEO is investigated. Note that, breaking either path, there is a complete single-loop OEO, which is able to run freely by adjusting the loop gain. With SMF 2 broken, the measured microwave signals with frequency within the band of BPF is presented in Fig. 3(a). The zoom-in-view of the spectrum of the signal is demonstrated in Fig. 3(b). Fig. 3 shows that generated signal has many harmonics with the same frequency separation and the FSR is about 301.5 KHz. With SMF 1 broken, the measured microwave signals with frequency within the band of BPF is shown in Fig. 3(c). The zoom-in-view of the spectrum of the signal is measured in Fig. 3(d). The FSR is 309 KHz. Fig. 3(e) and (f) illustrates the signal spectrum and zoom-in-view of the dual-loop OEO. As expected, an obvious Vernier effect is generated. In order to get the upper envelop curve of the signal, empirical mode decomposition (EMD) algorithm is applied to the extreme points of the measured frequency

This article has been accepted for publication in a future issue of this journal, but has not been fully edited. Content may change prior to final publication. Citation information: DOI 10.1109/JPHOT.2021.3119960, IEEE Photonics Journal

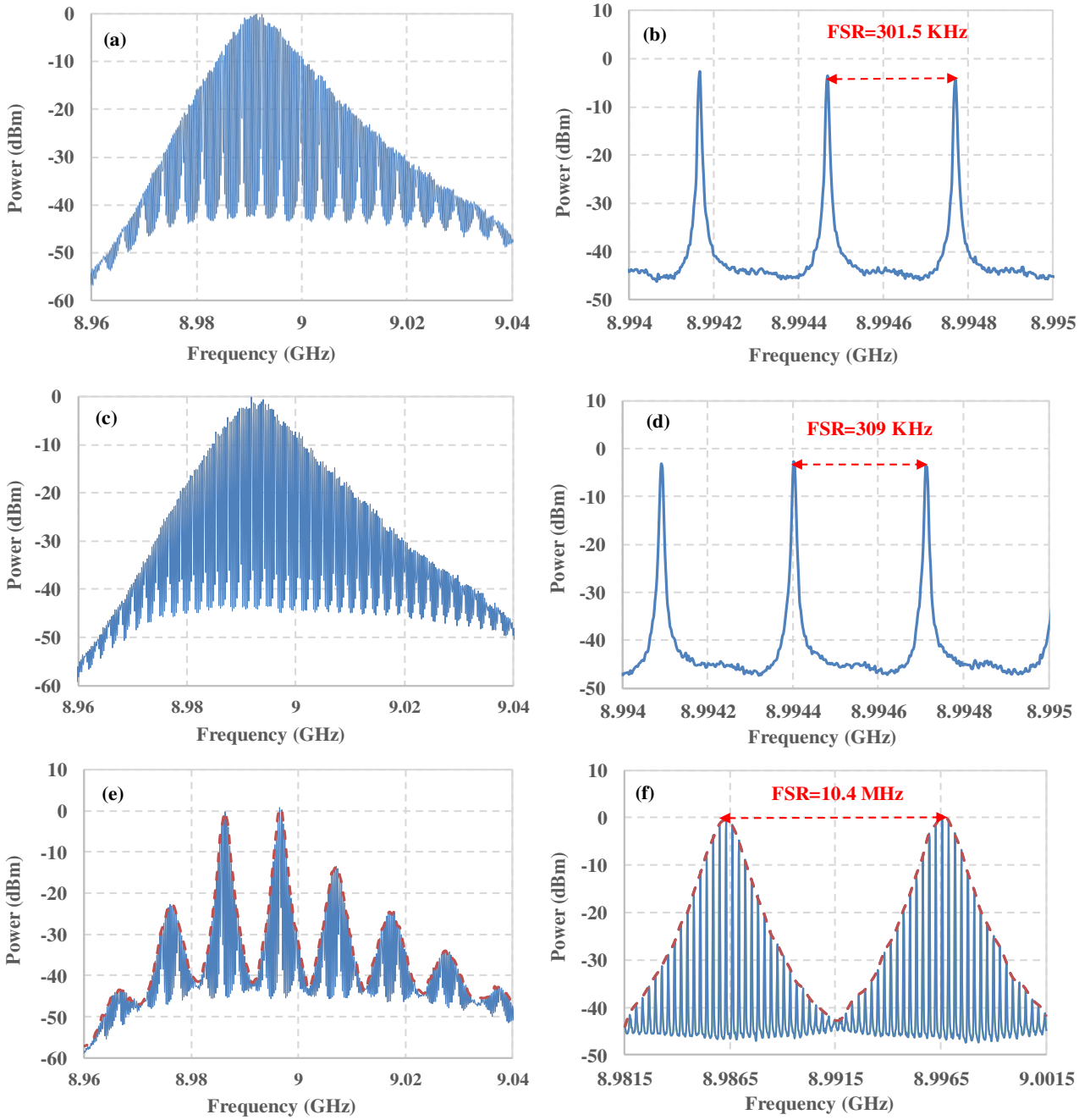

Fig. 3. Electrical spectrum of the generated microwave signals. (a) single-loop OEO with SMF 2 broken; (b) Zoom-in-view of the signal; (c) single-loop OEO with SMF 1 broken; (d) Zoom-in-view of the signal; (e) dual-loop OEO; (f) Zoom-in-view of the signal;

response curves, showing in red dotted line in Fig. 3. (e) and (f). The FSR of the dual-loop OEO is extended to 10.4 MHz, which is much larger than that of single-loop OEO and is agreed with the theoretical estimated about 10.96 MHz. As can be seen, the width of the spectrum envelop of the dual-loop OEO is much wider than the mode-width of the single-loop OEO, which may introduce more error in the determination of the center frequency. Therefore, to accurately obtain the peak frequency of the envelope, a signal analysis method (EMD) was applied to get the envelop curve of the dual-loop OEO. The error can also be reduced by employing curve fitting method and averaging method. Moreover, due to the higher sensitivity of the dual-loop system, even high measurement error of center frequency shift can only correspond to tiny strain change. Therefore, the strain measurement error caused by the widening of the spectrum envelop is negligible.

Finally, the relationships between the frequencies of the tracking signal both in single-loop OEO and dual-loop OEO and the axial strain are measured. With the SMF 2 broken, the harmonic frequency at 8.99988 GHz is choose as the tracking signal. To test the hysteresis of the interrogation system, the frequencies of the tracked microwave signal with both increasing and decreasing the axial strain are recorded at room temperature, showing in Fig. 4 (a) and (b). We can that, with

This article has been accepted for publication in a future issue of this journal, but has not been fully edited. Content may change prior to final publication. Citation information: DOI 10.1109/JPHOT.2021.3119960, IEEE Photonics Journal

the increase of axial strain, the tracking signal shifts to the higher frequency range, while the tracking signal shifts to the lower frequency range with the decrease of axial strain. Fig. 4(c) depicts the tracking signal as a function of the axial strain. Seen from Fig. 4 (c), the sensitivity by linearly fitting the measured data is 0.31 KHz/με.

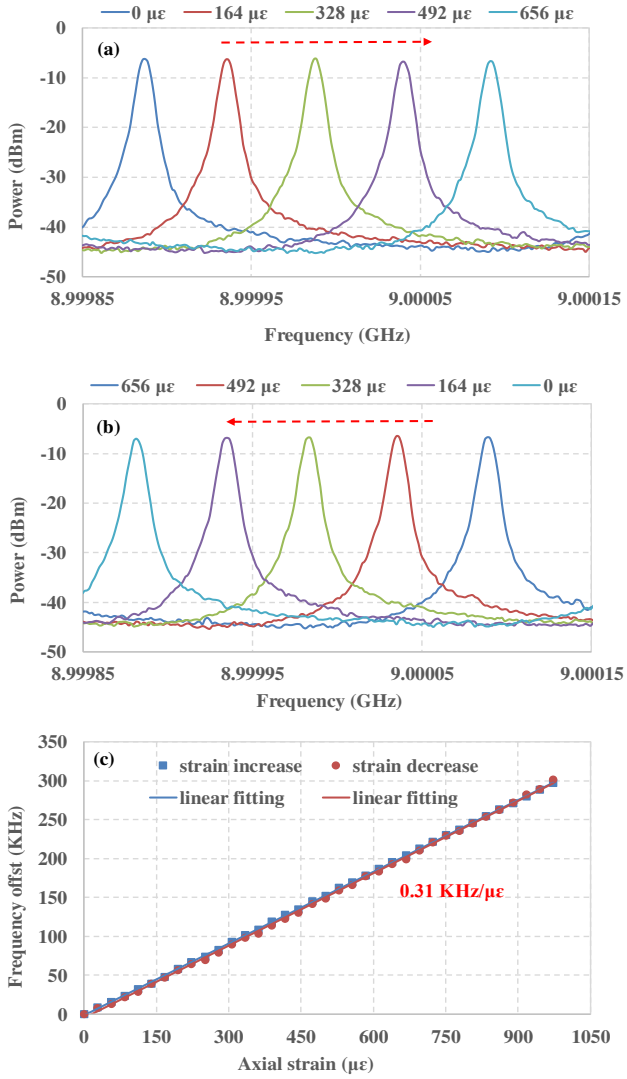

Fig. 4. Superposed electrical spectrum of single-loop OEO at different axial strain. (a) axial strain increase; (b) axial strain decrease; (c) the relationship between the frequency shift of the tracking signal and axial strain.

With SMF 1 and SMF 2 both connected, the frequency shift of envelop of dual-loop OEO with the axial strain is measured. The harmonic frequency at 8.9996 GHz is choose as the tracking signal. Fig. 5. (a) and (b) show the superposed spectrum of tracking signal at different axial strain. As can be seen from Fig. 5(a) and (b), the tracking signal shifts to a low (high) frequency range as the axial strain increases (decreases), which is agreed with the Eq. (11). Fig. 5(c) illustrates the measured tracking signal as a function of the axial strain. The sensitivity by linear fitting the measured data is -11 KHz/με. Compared with the result based on single-loop OEO, the sensitivity of the sensor based on dual-loop OEO have been magnified about 35 times, which agreed with predicated value of 36 times and demonstrates that the Vernier effect is an effective way to improve the sensing sensitivity.

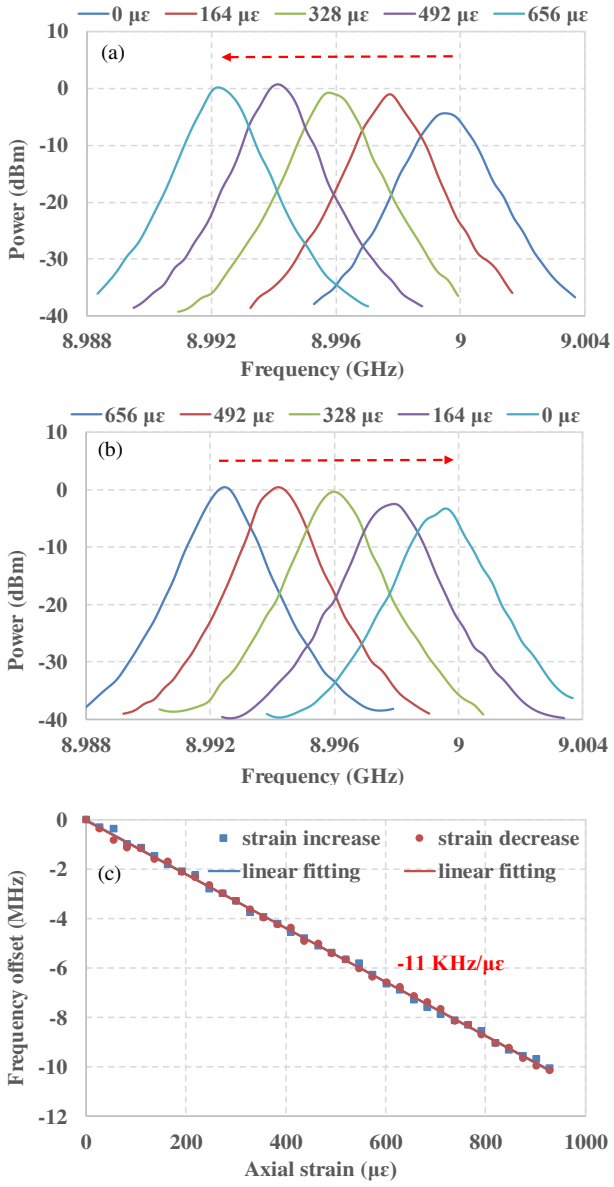

Fig. 5. Superposed envelop electrical spectrum of dual-loop OEO at different axial strain. (a) axial strain increase; (b) axial strain decrease; (c) the relationship between the frequency shift of the tracking signal and axial strain.

The resolution and measurement range of the proposed strain sensor is evaluated. In an ideal situation, the resolution of the sensing system is limited by the frequency measurement resolution (~1Hz) of the ESA for a fixed sensitivity. In this system, the sensitivity is 0.31 KHz/με for single-loop OEO. Therefore, the resolution is theoretically calculated to be 3×10^{-3}με. For dual loop OEO, the sensitivity is -11KHz/με. Therefore, the resolution is theoretically calculated to be 9×10^{-5} με. But in practice, the resolution is also affected by the stability of the OEO. The measurable range of the strain sensor is limited by the free spectrum range (FSR) of the OEO to avoid frequency ambiguity. In our experiment, the FSR of the single-loop OEO is 301.5 KHz. Considering the sensitivity of 0.31 KHz/με, the

This article has been accepted for publication in a future issue of this journal, but has not been fully edited. Content may change prior to final publication. Citation information: DOI 10.1109/JPHOT.2021.3119960, IEEE Photonics Journal

measurement range is restricted to be 972 με. The FSR of the dual-loop OEO is about 10.4 MHz with a sensitivity of -11 KHz/με. As a result, the measurement is restricted to be 945 με. It can be seen that the dual-loop structure hardly affects the measuring range. It should also be noted that if we track the change of the FSR value rather than the center frequency, the measurable range of this proposed method can be considered as unlimited because there is a one-to-one correspondence between the value of the FSR and the strain.

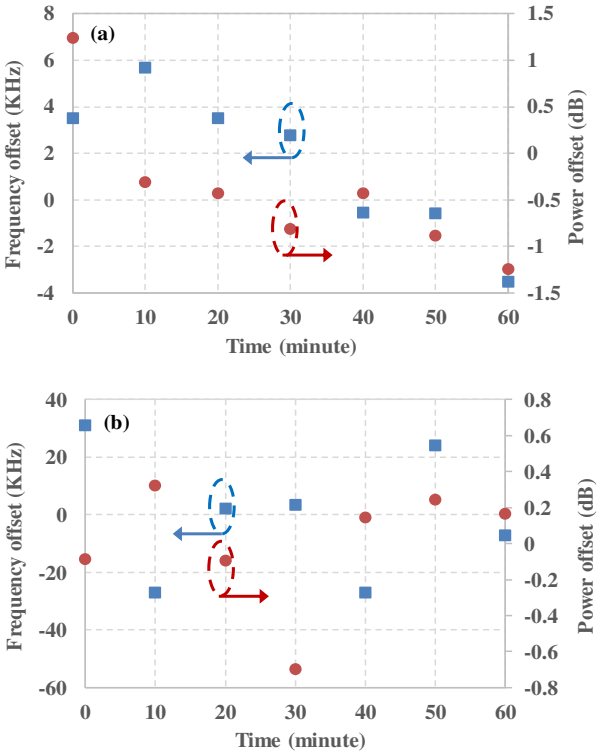

Fig. 6. The stability of the oscillating frequency at a constant axial strain; (a) signal-loop OEO; (b) dual-loop OEO.

Besides, the stability of the oscillating frequency is a critical parameter for high precision measurement. Hence, we set the proposed sensor operating at room temperature for a period of an hour when a constant axial strain is applied to the sensing FBG. The frequencies of single-loop and dual-loop OEO are recorded for 60 minutes with a step of 10 minutes, which are shown in Fig. 6 (a) and (b), respectively. As can be seen that the maximum frequency variation of single-loop OEO is around ±4.5 KHz, which corresponds to ±14.5 με axial strain measurement error. The maximum frequency variation of dual-loop OEO is around ±30 KHz, which correspond to ±2.7 με axial strain measurement error. The power variation of single-loop OEO and dual-loop OEO are around ±1.3 dB and ±0.45 dB, respectively. It indicates that the Vernier effect is an effective way to reduce the measurement errors both of frequency and power.

It should be noted that the stability of the OEO can normally be improved by using a dual-loop configuration. However, the frequency variation of the dual-loop OEO is even higher than that of the singe-loop OEO according to Fig.6 (a) and (b). This is because that our configuration is quite different from the traditional dual-loop ones. In a traditional dual-loop configuration, a very long loop and a short loop are configured, and a narrowband RF filter is added to achieve a stable single-mode oscillation with low-phase noise. However, to achieve obvious Vernier effect, the length of the two loops are very close and none RF filter is used in our proposed configuration. Thus, the proposed dual-loop OEO is approximately equal to two signal-loop OEO with the same loop length in parallel. Moreover, due to the higher sensitivity of the dual-loop OEO to the environment, the frequency variation of the proposed dual-loop OEO is even higher than that of signal-loop OEO.

Finally, it is known that the initial oscillation microwave signals of the OEO are originated from noise. The oscillation needs to build up repeatedly from the optical and electrical gain spectra for each new frequency component, which will take some building time. According, the capability for dynamic stain sensing is limited by the building time of the OEO. Normally, the building time of the OEO depends on the length of the loop. In our experiment, the length of the whole loop is less than 1 km and the building time is in 10 microseconds. Therefore, the proposed sensing system could have a good response to the dynamic strain signal with a frequency up to 100 kHz.

IV. Conclusion

In conclusion, an OEO based FBG sensor with an improved scale factor employing Vernier effect has been proposed and experimentally demonstrated. The Vernier effect is successfully achieved by adopting suitable length different of two loops at different wavelengths. The experimental results indicated that the frequency of the tracking microwave signal has a good linear relationship with the FBG resonance wavelength as well as the axial strain applied to the FBG. With the help of Vernier effect, the sensitivity has been improved 35 times from 0.31 KHz/με in single-loop OEO to -11 KHz/με in dual-loop OEO. Furthermore, the measurement error has been reduced from ±14.5 με to ±2.7 με. The proposed method has potential application for high precision axial strain, temperature and other FBG based sensors. Besides, the sensitivity can be further increased by adjusting the length difference between loop 1 and loop 2 or employing DCF with larger dispersion coefficient.

References

[1] Y. Rao, “In-fiber Bragg grating sensors,” *Meas. Sci. Technol.*, vol. 8, no. 4, pp. 355–375, Aug. 1997.

[2] A. D. Kersey, M. A. Davis, H. J. Patrick, M. LeBlanc, K. P. Koo, C. G. Askins, M. A. Putnam, and E. J. Friebele, “Fiber grating sensors,” *J. Lightwave. Technol.*, vol. 15, no. 8, pp. 1442–1463, Aug. 1997.

[3] X. S. Yao and L. Maleki, “Optoelectronic microwave oscillator,” *J. Opt. Soc. Am. B*, Vol. 13, no. 8, pp. 1725–1735, Aug. 1996.

[4] J. Yao, “Optoelectronic Oscillator for High Speed and High Resolution Optical Sensing,” *J. Lightwave. Technol.*, vol. 35, no. 16, pp. 3489-3497, Aug. 2017.

[5] J. Yao, “Microwave Photonic Sensors,” *J. Lightwave. Technol.*, Vol. 1, no. 1, pp. 99, Dec. 2020.

[6] X. Zou, M. Li, W. Pan, B. Luo, L. Yan, L. Shao, “Optical length change measurement via RF frequency shift analysis of incoherent light source based optoelectronic oscillator,” *Opt. Express*, vol. 22, no. 9, pp. 11129-11139, May, 2014.

[7] Y. Wang, J. Zhang, and J. Yao, “An Optoelectronic Oscillator for High Sensitivity Temperature Sensing,” *IEEE Photonics Technol. Lett.*, vol. 28, no. 13, pp. 1458–1461, Jul. 2016.

[8] L. Liu, H. Gao, T. Ning, L. Pei, J. Zheng, J. Li and J. Xu, "High accuracy temperature sensing system exploiting a Sagnac interferometer and an optoelectronic oscillator," *Opt. Laser Technol.,* vol. 123, pp. 105951, Mar. 2020.

[9] L. D. Nguyen, K. Nakatani, and B. Journet, "Refractive Index Measurement by using an optoelectronic oscillator," *IEEE Photonics Technol. Lett.*, vol. 22, no. 12, pp. 857–859, Jun. 2010.

[10] Q. Shi, Y. Wang, Y. Cui, W. Xia, D. Guo and M. Wang, "Resolution-enhance fiber grating refractive index sensor based on an optoelectronic oscillator," *IEEE Sens. J.* vol. 18, no. 23, pp. 9562-9567, Dec. 2018.

[11] Y. Yang, M. Wang, Y. Shen, Y. Tang, J. Zhang, Y. Wu, S. Xiao, J. Liu, B. Wei, Q. Ding, and S. Jian, "Refractive Index and Temperature Sensing Based on an Optoelectronic Oscillator Incorporating a Fabry–Perot Fiber Bragg Grating," IEEE Photonics J., vol. 10, no. 1, pp. 1-9, Feb. 2018.

[12] Y. Wang, M. Wang, W. Xia, X. Ni and D. Wu, "Optical Fiber Bragg Grating Pressure Sensor Based on Dual-Frequency Optoelectronic Oscillator," *IEEE Photonics Technol. Lett.*, vol. 29, no. 21, pp. 1864-1867, Nov. 2017.

[13] B. Yin, M. Wang, S. Wu, Y. Tang, S. Feng and H. Zhang, "High sensitivity axial strain and temperature sensor based on dual-frequency optoelectronic oscillator using PMFBG Fabry-Perot filter," *Opt. Express*, vol. 25, no. 13, pp. 14106-14113, Jun. 2017.

[14] O. Xu, J. Zhang, H. Deng and J. Yao, "Dual-frequency Optoelectronic Oscillator for Temperature-Insensitive Interrogation of a FBG Strain Sensor," *IEEE Photonics Technol. Lett.*, vol. 29, no. 4, pp. 357-360, Feb. 2017.

[15] W. Wang, Y. Liu, X. Du, X. Zhong, C. Yu and X. Chen, "Ultra-Stable and Real-Time Demultiplexing System of Strong Fiber Bragg Grating Sensors Based on Low-Frequency Optoelectronic Oscillator," *J. Lightwave. Technol.*, vol. 38, no. 4, pp. 981–988, Feb. 2020.

[16] Z. Xu, X. Shu, and H. Fu, "Fiber Bragg grating sensor interrogation system based on an optoelectronic oscillator loop," *Opt. Express*, vol. 27, no. 16, pp. 23274-23281, Aug. 2019.

[17] D. Feng, Y. Gao, T, Zhu, M. Deng, X. Zhao and K. Li, "High-precision Temperature-compensated Magnetic Field Sensor based on Optoelectronic Oscillator," *J. Lightwave Technol.*, vol. 39, no. 8, pp. 2559-2564, Apr. 2021.

[18] Y. Chen, Y. Wang, Z. Song, J. Lei, "High-sensitivity optical fiber temperature sensor based on a dual-loop optoelectronic oscillator with the Vernier effect," *Opt. Express*, vol. 28, no. 23, pp. 35264-35271, Nov. 2020.

[19] Z. Xu, Q. Sun, B. Li, Y. Luo, W. Lu, and D. Liu, "Highly sensitive refractive index sensor based on cascaded microfiber knots with Vernier effect," *Opt. Express*, vol. 23, no. 5, pp. 6662–6672, Mar. 2015.

[20] P. Zhang, M. Tang, F. Gao, B. Zhu, and S. Fu, "Cascaded fiber-optic Fabry-Perot interferometers with Vernier effect for highly sensitive measurement of axial strain and magnetic field," *Opt. Express*, vol. 22,no. 16, pp. 19581–19588, Aug. 2014.

Xiaozhong Tian received the B. E. and M. S. degrees from Harbin Engineering University, Harbin, China, in 2010 and 2013, respectively. He is currently working toward the Ph. D. degree in physical electronics with the School of Computer and Electronic Information, Nanjing Normal University, Nanjing, China. His research interests include microwave photonics, optoelectronic oscillators and optical fiber sensors.

Jingzhan Shi received the B.S., the M.S., and the Ph.D. degrees in communication and information system from the Nanjing University of Aeronautics and Astronautics, Nanjing, China, in 2013, 2016, and 2020, respectively. He is currently a lecturer with the School of Computer and Electronic Information, Nanjing Normal University, Nanjing, China. His current research interest is in microwave photonics measurement.

Yiping Wang received the B.E. and Ph.D degrees in school of electronic science & engineering from Southeast University, Nanjing, China, in 2002 and 2007, respectively. He joined Nanjing Normal University, Nanjing, China in 2007 and is now working as a Professor at the School of Computer and Electronic Information in this University. In February 2015, he joined the Microwave Photonics Research Laboratory, School of Electrical Engineering and Computer Science, University of Ottawa, Ottawa, ON, Canada, as a visiting scholar for one year. His current research interests include optical fiber sensor and microwave photonics sensing technology. He has published more than 40 international conference and top-level journal papers.

Le Li received the B. E. degree from Anhui University of Technology, Ma'anshan, China, in 2020. Now he is studying for the M. S. degree in Electronic and Communication Engineering at the School of Computer and Electronic Information, Nanjing Normal University, Nanjing, China. He is engaged in the research of optoelectronic oscillators and optical fiber sensor.

Yun She received the B. E. degree from Nanjing Normal University Zhongbei College, Nanjing, China, in 2019. She is currently working toward the M. S. degree in electronic science and technology with the School of Computer and Electronic Information, Nanjing Normal University, Nanjing, China. Her research interests include microwave photonics, microwave photonic filter and optical fiber sensors.